has a smaller bond-angle distortion than the other materials. This result is understandable in view of the greater hardness of diamond, resulting from an increased stiffness of the tetrahedral bond angle. The bond-bending force constants for crystalline diamond, silicon and germanium are in the ratio 4·9:0·44:0·37 (Tomassini, Amore Bonapista, Lapiccirella, Lodge & Altmann, 1987), as determined by fitting lattice-dynamical results from neutron diffraction data.

The authors acknowledge financial support from the Australian Research Grants Committee without which development of the technique would not have been possible. The extensive assistance of D. Dwarte and Dr Z. Liu in developing and applying the techniques is acknowledged, and M. Lake is thanked for permission to refer to his work on Pt and alloys of Si and F. The specimen of glassy carbon was kindly supplied by Dr S. Prawer.

References

ANSTIS, G. R., LIU, Z. & LAKE, M. R. (1988). *Ultramicroscopy.* In the press.

BRIGHAM, E. O. (1974). *The Fast Fourier Transform.* Englewood Cliffs, New Jersey: Prentice Hall.

DOYLE, P. A. & TURNER, P. S. (1968). *Acta Cryst.* A**24**, 390-397.

EGERTON, R. F. (1986). *Electron Energy Loss Spectroscopy in the Electron Microscope.* New York: Plenum

GRACZYK, J. F. (1979). *Phys. Status Solidi. A*, **55**, 231-242.

GRACZYK, J. F. & MOSS, S. C. (1969). *Rev. Sci. Instrum.* **40**, 424-433.

GRIGOROVICI, R. (1973). In *Electronic and Structural Properties of Amorphous Semicondutors*, edited by P. G. LE COMBER & J. MORT, pp. 191-241. London: Academic Press.

GRIGSON, C. W. B. (1962). *J. Electron. Control*, **12**, 209-232.

JENKINS, G. M. & KAWAMURA, K. (1976). *Polymeric Carbons - Carbon Fibre, Glass and Char.* Cambridge Univ. Press.

KAPLOW, R., STRONG, S. L. & AVERBACH, B. L. (1965). *Phys. Rev.* **138**, A1336-A1345.

KEATING, D. T. (1963). *J. Appl. Phys.* **34**, 923-925.

KONNERT, J. H. & KARLE, J. (1973). *Acta Cryst.* A**29**, 702-710.

LAKE, M. R. (1988). PhD thesis. Univ. of Sydney, Australia.

MCKENZIE, D. R., COCKAYNE, D. J. H., DWARTE, D. M. & TURNER, P. S. (1988). *Philos. Mag. B.* Submitted.

MCKENZIE, D. R., MARTIN, P. J., WHITE, S. B., LIU, Z., SAINTY, W. G., COCKAYNE, D. J. H. & DWARTE, D. M. (1987). *Proc. E-MRS Meet.*, June 1987, pp. 203-206. Paris: Les Editions de Physique.

MOSS, S. C. & GRACZYK, J. F. (1969). *Phys. Rev. Lett.* **23**, 1167-1171.

REIMER, L. (1984). *Transmission Electron Microscopy.* Berlin: Springer.

SAINTY, W. G., MCKENZIE, D. R., MARTIN, P. J., NETTERFIELD, R. P., COCKAYNE, D. J. H. & DWARTE, D. M. (1988). *J. Appl. Phys.* In the press.

TOMASSINI, N., AMORE BONAPISTA, A., LAPICCIRELLA, A., LODGE, K. W. & ALTMANN, S. (1987). *J. Non-Cryst. Solids*, **93**, 241-256.

WARREN, B. E. (1969). *X-ray Diffraction.* Reading, MA: Addison-Wesley.

WYCKOFF, R. W. G. (1963). *Crystal Structures.* New York: Interscience.

Acta Cryst. (1988). A**44**, 878-884

Validity Domain of the Weak-Phase-Object Approximation for Electron Diffraction of Thin Protein Crystals

MING-HSIU HO* AND BING K. JAP

Division of Biology and Medicine, Lawrence Berkeley Laboratory, University of California, Berkeley, CA 94720, *USA*

AND ROBERT M. GLAESER†

Department of Biophysics and Medical Physics, and Division of Biology and Medicine, Lawrence Berkeley Laboratory, University of California, Berkeley, CA 94720, *USA*

(*Received* 30 *November* 1987; *accepted* 9 *March* 1988)

Abstract

The domain of validity of the weak-phase-object (WPO) approximation is evaluated for high-energy electrons (100 keV, 500 keV and 1 MeV) scattered by crystalline biological macromolecules. Cytochrome b_5 is used as an example in which calculated dynamical diffraction intensities are used to simulate observed diffraction intensities, which are then compared with intensities calculated by the weak-phase-object approximation. Three criteria of validity are used, namely the crystallographic residual (R value), the interpretability of difference Patterson maps, and the results of phasing by the heavy-atom isomorphous replacement method. The present calculations indicate that the error associated with the WPO approxi-

* Current address: Intermediate Voltage Electron Microscopy and Biomedical Image Analysis Resource, Department of Biology, University of Pennsylvania, Philadelphia, PA 19104, USA.

† To whom reprint requests should be addressed.

0108-7673/88/060878-07$03.00

mation is quite acceptable up to a specimen thickness of 200 Å for 100 keV electrons, which is two to four times the thickness limit for crystalline organic structures with much smaller unit-cell dimensions. An equally acceptable thickness limit at 500 keV and 1 MeV is about 300–350 Å.

Introduction

Electron crystallography, which involves both diffraction and direct imaging with very thin crystals, is becoming an increasingly important method of structure analysis for biological macromolecules (Amos, Henderson & Unwin, 1982; Glaeser, 1985). Diffraction data up to a resolution of 1·8 Å have been obtained from a protein crystal (Chiu, 1982), and images have been used to obtain accurate phases to a resolution of 3·5 Å (Jeng, Chiu, Zemlin & Zeitler, 1984; Henderson, Baldwin, Downing, Lepault & Zemlin, 1986). Interpretation of images and diffraction intensities for biological materials normally uses the weak-phase-object (WPO) approximation. The approximation assumes that electron diffraction of macromolecules is limited to single scattering. Furthermore, the approximation assumes a flat Ewald sphere, and thus it is valid only for very high incident energy where the electron wavelength is small compared with the available resolution. However, such assumptions can be expected to be increasingly invalid for increasingly greater specimen thickness and higher resolution. Although there has been some theoretical analysis of the limits of validity of the weak-phase-object approximation for small organic molecules (Ishizuka & Uyeda, 1977; Dorset, Jap, Ho & Glaeser, 1979; Jap & Glaeser, 1980) or negatively stained protein crystals (Dorset, 1984), there have not yet been any published calculations relating to unstained crystalline proteins or other macromolecules of similarly complex structure.

We have carried out dynamical diffraction calculations for cytochrome b_5 to determine the domain of validity of the WPO approximation as a function of accelerating voltage, specimen thickness and structural resolution. The initial results show that it is generally valid to use the WPO approximation to interpret diffraction intensities up to a thickness of 200 Å or more at 100 keV, and up to a thickness of 350 Å at 500 keV or 1 MeV. A new observation made in the course of this work is that the dynamical calculations produce a systematic redistribution of diffraction intensities, even when the specimen thickness is small enough to produce otherwise only minor dynamical effects. This redistribution has an effect similar to that of the temperature factor when the intensities are displayed on a Wilson plot. The corresponding 'apparent' thermal Debye parameters seem to reach a limiting value of B which fluctuates between 9 and 10 $Å^2$. Correction for this 'apparent' temperature factor was carried out in all cases.

Methods

Cytochrome b_5 ($M_r = 11\,000$) was chosen as a model structure for our numerical calculations. The structure has been determined from X-ray diffraction studies (Mathews, Levine & Argos, 1972), and the atom coordinates are available from the Protein Data Bank of Brookhaven National Laboratory. Cytochrome b_5 grows in the orthorhombic space group $P2_12_12_1$, with unit-cell dimensions $a = 64·54$, $b = 46·04$ and $c = 29·91$ Å. The short c-axis repeat distance was taken to be the slice thickness in the computation of the diffracted wave, in the multislice formulation. The basic theoretical formulation for the multislice dynamical theory is as described previously (Cowley & Moodie, 1957; Jap & Glaeser, 1978), and the calculations were carried out with computer programs similar to those used previously for less-complex organic structures (Jap & Glaeser, 1980), but with the convolution operation being performed by multiplication in Fourier space.

Structure factors for crystalline cytochrome b_5 were calculated to a resolution of 0·8 Å with the atomic structure factors given in parametric form by Doyle & Turner (1968). Hydrogen atoms were not included in the calculation. All atom positions were assumed to be stationary, and no thermal motion or other type of structural disorder was incorporated into the calculations. The effect of partial occupancy of heavy atoms in derivatives was modeled by replacing the actual heavy atoms by effective atoms at full occupancy whose atomic number was reduced in proportion to the fractional occupancy. The projected potential which is needed for the multislice dynamical calculations was obtained by taking the inverse Fourier transform of the $hk0$ structure factors.

The use of all diffracted beams to a resolution of 0·8 Å, involving 23 893 beams in the $hk0$ net, ensured that a sufficient number of reflections were included such that the summed total of the calculated dynamical diffraction intensities was never less than 0·997 of the incident intensity, even up to a thickness of 930 Å. All calculations were limited to the case in which the incident wave vector is parallel to the crystal c axis. Three different accelerating energies, 100, 500 and 1000 keV, were used in the calculation. Fig. 1 shows representative examples of diffraction intensities calculated at 100 keV for two different resolutions, corresponding to Miller indexes of 200 and 1,21,0, respectively. The corresponding intensities calculated by using the WPO approximation increase as H^2, the square of the thickness. This quadratic increase occurs simultaneously for all reflections because the Ewald sphere is assumed to be flat in the WPO approximation, *i.e.* the WPO

approximation incorporates within it a 'zero-wavelength' approximation. The calculated Cowley-Moodie diffraction intensities, like the real experimental intensities, effectively retain the curvature of the Ewald sphere. In this case, then, as the specimen thickness increases, and the widths of the (kinematic) diffraction maxima along the reciprocal-lattice rods become smaller and smaller, successive minima and maxima must pass through the intersection of the stationary curved Ewald sphere and the reciprocal-lattice rod. The effect is greatest, of course, at the highest resolution.

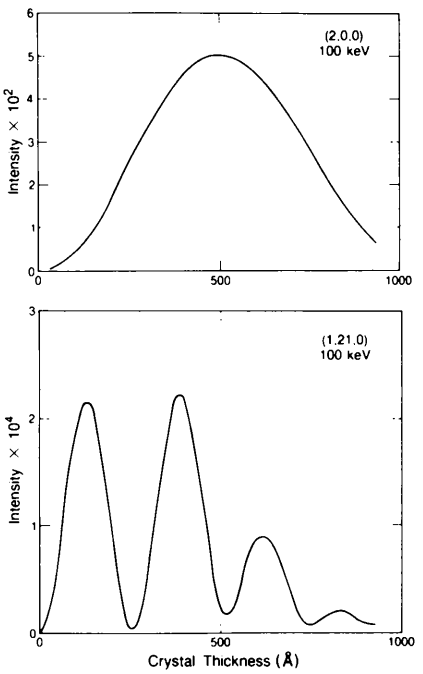

Fig. 1. The Cowley-Moodie multislice dynamical intensities for the 200 and 1,21,0 reflections of cytochrome b_5 are plotted as a function of crystal thickness.

To make our simulation as close as possible to the real experimental situation, the dynamical intensities were scaled according to the scheme commonly used by X-ray crystallographers when scaling together diffraction data for both native and heavy-atom-derivative protein crystals. This scaling is achieved by the use of Wilson plots (Wilson, 1942). Our goal in using the Wilson plot has only been to treat the data (*i.e.* calculated simulations) in the same way that would normally be the case for kinematic data, and in so doing to establish the limitations of resolution and specimen thickness for which such a treatment remains valid, up to a specified degree of error. It has not been our goal to convert dynamical diffraction intensities to (kinematic) structure factors by an analysis of Wilson plots, as is proposed in the work of Li (1963). It should again be noted that, in our calculations of the dynamical intensities, all atoms are assumed to be stationary and no thermal disorder is introduced in the calculation.

Results

The dynamical intensities exhibit an apparent temperature factor, as can be seen from the Wilson plots shown in Fig. 2 for accelerating voltages of 100 and 500 kV. For the WPO approximation, in the absence of thermal (or other) disorder, the diffraction intensities must be scattered about a horizontal line. At very small thicknesses, *e.g.* 30 Å, the dynamical intensities also show the expected absence of a temperature factor. However, for a specimen thickness of 300 Å, the slope of the Wilson plot is quite steep, corresponding to an apparent thermal Debye parameter B of ~ 9 Å^2 for 100 keV electrons and ~ 10 Å^2 for 500 keV electrons. These numbers seem

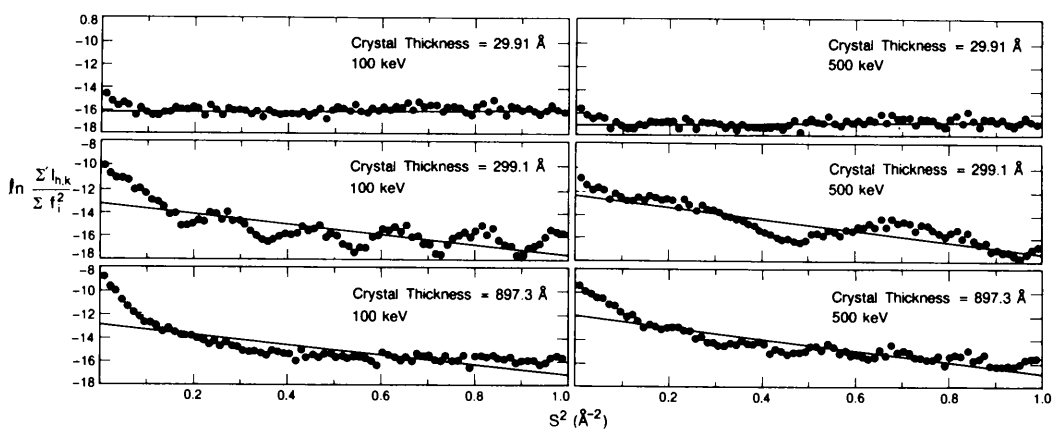

Fig. 2. Wilson plots for the dynamical electron diffraction intensities calculated for cytochrome b_5 at different values of the specimen thickness and electron accelerating voltage, as indicated. The notation $\sum$ refers to summation over restricted annular zones in reciprocal space, and f_i represents the atomic scattering factors. The slopes and y intercepts of the straight lines are determined as a least-squares best fit to the calculated data.

Table 1. *The 'apparent' thermal Debye parameter, B (Å^2), determined from the slopes in the Wilson plots*

Thickness (×29·91 Å)	100 keV	500 keV	1·0 MeV
1	−0·22	−0·21	−0·21
2	10·24	0·71	0·11
3	6·90	2·47	0·68
4	9·50	5·54	1·53
5	7·90	10·19	2·73
10	8·97	10·17	9·54
15	9·33	10·35	8·73
20	9·38	10·42	9·12
25	9·22	10·40	9·61
30	9·37	10·49	9·57

The relation between B and the root mean square atomic displacement, u, is $B = 8\pi^2\overline{u^2}$.

to level off at values between 9 and 10 at high thickness values, regardless of the accelerating voltage (Table 1). Such values of the thermal Debye parameter correspond to an effective r.m.s. atomic displacement of 0·34–0·36 Å. The expected fluctuations in the average structure factor for different annular zones in resolution are also more pronounced for greater specimen thickness (Fig. 2).

The mathematical or physical basis for the apparent temperature factor is not clear. One factor that could be involved, but which we have not yet investigated, is a direct consequence of curvature of the Ewald sphere. If we consider first of all the kinematic case, with the incident wave vector perpendicular to the plane of a thin protein crystal, the Ewald sphere will sample the Fourier transform with progressively larger excitation error at increasingly higher resolution. The resulting diffraction intensities will therefore be progressively weaker than the peak intensities as the resolution increases. Qualitatively, the effect just discussed should have the same behavior as would be produced by a finite thermal Debye parameter. A similar effect would not be expected to appear in real experimental data, however, because there one measures integrated diffraction intensities, for which the Ewald sphere has been swept through the finite width of the diffraction spot, rather than merely sampling the Fourier transform for a single incident-beam direction. In the dynamical case we can again expect to see a 'temperature-factor' effect arising from curvature of the Ewald sphere, since the Cowley–Moodie formulation does incorporate Fresnel propagation of the wave within the finite thickness of the specimen. However, the effect in the dynamical case cannot be pictured as intuitively as in the kinematic case, because the simple Fourier-transform relationship between the crystal thickness and the sampled diffracted wave is no longer valid.

In the work reported here it has been impractical, in terms of available computer costs, to calculate dynamical intensities that have been integrated over a significant range of excitation errors. Had we been able to do so, we anticipate that the 'temperature-factor effect' seen when using Wilson plots would be much smaller, or might not even occur. As a practical expedient at this stage, all of the calculated dynamical diffraction intensities were simply corrected for the apparent temperature factor as part of a routine scaling procedure, before they were then used to calculate R factors or difference Patterson maps.

As a first test for the onset of significant dynamical effects, we have computed the R-factor residual between the WPO and dynamical diffraction amplitudes, designated as F_{WPO} (WPO F) and F_{CM} (Cowley–Moodie F) respectively. The R factor was calculated using all data up to a limiting resolution $S_{\max}$ and is defined by

$$R(S_{\max}) = \frac{\sum_{(h,k)}^{S_{\max}} \| F_{\mathrm{CM}}(h,k)| - N|F_{\mathrm{WPO}}(h,k)\|}{\sum_{(h,k)}^{S_{\max}} |F_{\mathrm{CM}}(h,k)|}$$

where the normalization factor N is defined from the equation

$$N^2 = \sum_{(h,k)}^{S_{\max}} |F_{\mathrm{CM}}(h,k)|^2 \Big/ \sum_{(h,k)}^{S_{\max}} |F_{\mathrm{WPO}}(h,k)|^2.$$

Fig. 3 shows two representative examples of how the R factor increases with thickness, for $S_{\max} = 1/1{\cdot}4$ and for $S_{\max} = 1/8{\cdot}6$ Å^{-1} at 100 keV, 500 keV and 1 MeV.

A family of such curves was then used to define the domain of specimen thickness and resolution for which the WPO approximation is valid, within certain tolerated limits, as determined by different specified

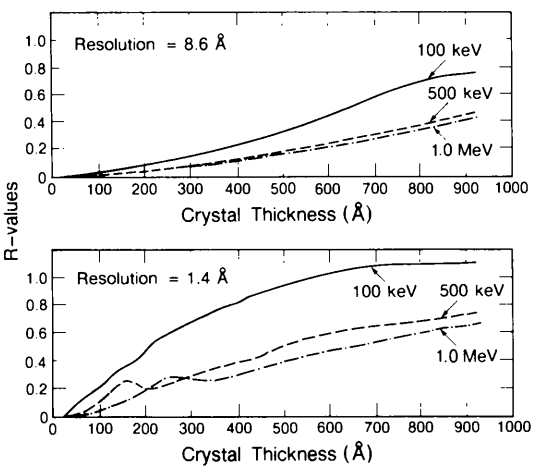

Fig. 3. Values of the R factor (see text for definition) between structure factors calculated for the weak-phase-object (WPO) approximation and the Cowley–Moodie multislice formulation. As the specimen thickness increases, the R factors increase. Such R factors also depend on the resolution limit (cut-off frequency).

values of the R factor. Fig. 4 shows smoothed curves that represent the boundaries of the domains of validity, for representative values of the R factor. Thus, for example, the curves in Fig. 4 show that, in the case of 100 keV electrons, the WPO approximation is valid to a thickness of 100 Å at a resolution of about 5 Å provided that one can tolerate an R factor, due solely to the inadequacy of the WPO approximation, of 0·05. If a higher R value can be tolerated, then the use of the WPO approximation remains valid to a larger thickness for the same resolution. As expected, the domain of validity increases as higher accelerating voltages are used. However, the difference between 500 keV and 1 MeV is not so significant when compared with the difference between 100 and 500 keV.

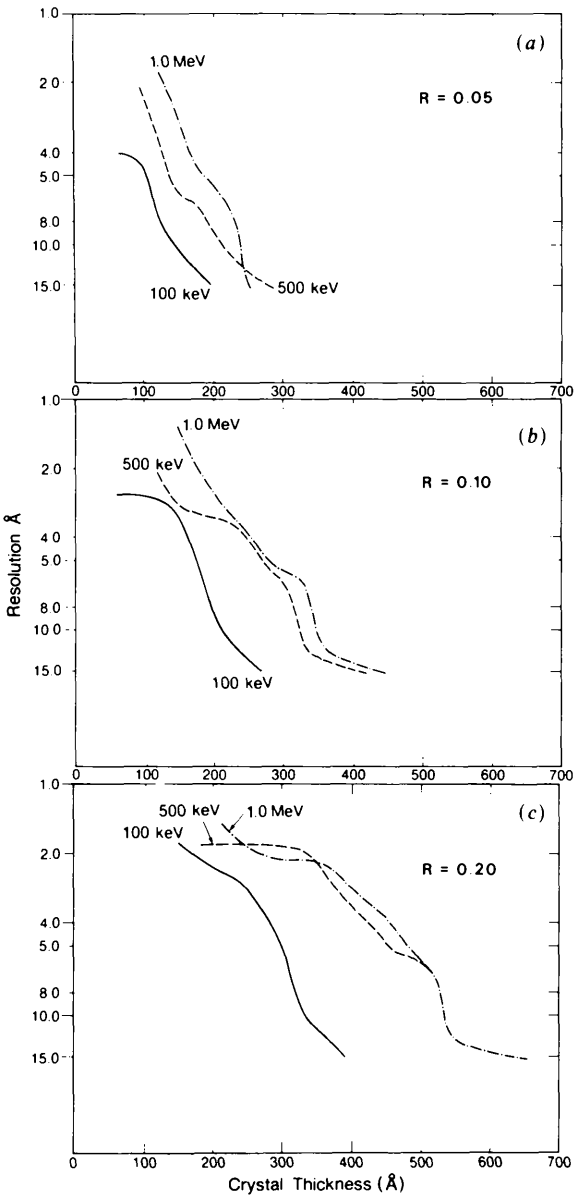

Fig. 4. The approximate domain of validity for the WPO approximation, using the criterion that the R factor should be less than (*a*) 0·05, (*b*) 0·10 or (*c*) 0·20. The various curves in each panel correspond to different electron accelerating voltages, as indicated.

The scaled dynamical diffraction intensities for native and heavy-atom-derivative protein crystals were used to generate difference Patterson maps by taking the Fourier transform of $(F_{PH} - F_P)^2$, where F_P is the modulus of the structure factor of the protein and F_{PH} is the structure-factor modulus of the protein plus heavy atoms. Fig. 5 shows the results derived using the structure factors limited to 3·5 Å for the electron voltages and thickness indicated. The contour levels of all the maps were 4, 7, 10, 16, 22, 28, 34, 40 after the peak at the origin was scaled to 100. Clearly, at the smallest simulated thickness the difference Patterson maps can be correctly interpreted. However, as the thickness increases, false peaks begin to emerge, and the relative values at each peak no longer represent the true occupancies.

The dynamical diffraction intensities for the native and heavy-atom-derivative protein crystals were next used to phase the $hk0$ reflections. Since this zonal projection is centrosymmetric, the phase choice is limited to 0 or π. The phases of the native structure

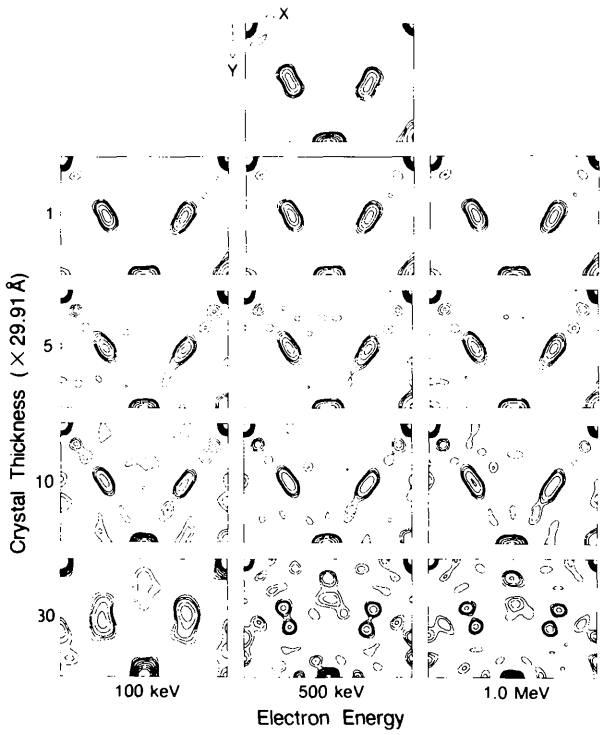

Fig. 5. Difference Patterson maps derived from the dynamical intensities of native and heavy-atom-derivative structures at various values of the crystal thickness and the electron voltage. For comparison, the autocorrelation map of the heavy-atom potential is shown at the top of this figure. All maps have been limited to a resolution of 3·5 Å, as stated in the text.

must therefore be taken to be the same as the phases of the heavy atoms alone, whenever the intensity of the derivative is larger than that of the native. When the intensity of the derivative is less than that of the native, then the phase of the native structure must be taken to be π plus the phase of the heavy atoms. The phases deduced in this way were compared with the correct phases, which are known from the model structure.

The results obtained in this phasing procedure are shown in Fig. 6. The upper three curves show the percentage of beams that are assigned wrong phases as a function of thickness, and the lower three curves represent the sum of their associated intensities as a percentage of the total diffracted intensity. For 100 keV electrons, at a thickness of 150 Å, about 10% of the diffracted beams were assigned the wrong phase. The 10% error rate occurs at about 240 Å for 500 keV and 1 MeV.

Discussion

The absolute accuracy of the present theoretical comparison is necessarily compromised by the decision to use a 30 Å slice thickness to calculate the dynamical diffracted waves. The principal reason for using the *c*-axis repeat distance as the slice thickness was to simplify the computation in order to reduce the computing costs. In addition to this practical consideration, however, we note that earlier calculations for simpler organic structures had already indicated that the kinematic approximation would be quite accurate for a specimen thickness of at least 50 Å (Jap & Glaeser, 1980; Dorset *et al.*, 1979). Thus it seems plausible to argue that the multislice formulation is not needed to describe wave propagation through the 30 Å of organic material involved in our present problem. We would like to point out that the use of too great a slice thickness is likely, if anything, to overestimate the dynamical effect, since it underestimates the 'spreading' of the diffracted wave due to the coupling of Fresnel propagation and multiple scattering.

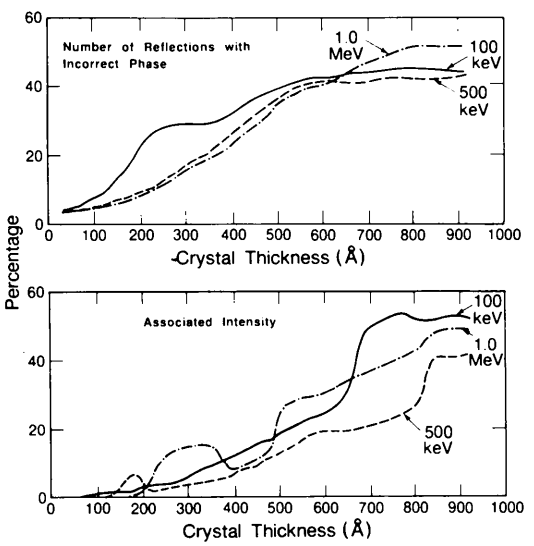

Fig. 6. The number of reflections that are assigned the wrong phase and their associated total intensities, as a precentage of all diffracted beams in the (*hk*0) plane, up to 2 Å resolution.

The results obtained in this work support the commonly held view that the WPO approximation provides a sufficiently accurate representation of electron-specimen interaction at 100 keV for thin unstained macromolecules. For specimens that are much thicker than 200 Å, however, the calculations indicate that substantial errors may arise from the use of the WPO approximation. The specimen thickness at which the WPO approximation can be safely used is increased by roughly a factor of 1·5 by going to high voltage.

The estimation of the number of phasing errors in Fig. 6 is intended to give only a rough idea of the thickness at which failure of the WPO approximation alone is likely to introduce a serious problem. A more accurate simulation of the limitations that will apply to phasing with real data would require that one also take into account the errors that arise when interpreting the difference Patterson function. As a preliminary guide, however, the results shown in Figs. 5 and 6 confirm the point that dynamical effects will not cause serious errors in interpretation up to a specimen thickness of 200 Å at 100 keV, and up to a specimen thickness of 350 Å at 500 keV or 1 MeV. A more sensitive test of the phasing problem would also require an examination of reflections in a non-centrosymmetric section of the reciprocal lattice. A quantitative evaluation of phasing errors that would result from the distorted Patterson function, and an investigation of non-centrosymmetric zones both represent important areas in which further investigation of the validity of the weak-phase-object approximation can be carried out.

By using the zero-wavelength approximation, an inherent discrepancy other than that associated with the single-scattering approximation exists between the WPO intensities and dynamical intensities, because the curvature of the Ewald sphere is not accounted for in the WPO approximation. Thus, for example, the domains of validity determined here do not provide completely accurate estimates for the limitations on the validity of the *kinematic* approximation. The domain of agreement between the kinematic approximation and dynamical theory should be at least as great as that of the WPO approximation. In particular, when curvature of the Ewald sphere is taken into consideration, high-resolution diffraction intensities will not increase quadratically with the thickness, as in the WPO approximation. Instead, they will reflect the progressive narrowing of the shape

function at reciprocal-lattice points, a result that can even cause the intensity to fall to zero when the Ewald sphere intersects a zero in the shape (thickness) transform. The same sort of effect is also built into the Cowley–Moodie formulation of dynamical theory, through inclusion of Fresnel wave propagation from one plane of the specimen to the next. Of course, the net effect in the dynamical case can be much more complex than in the kinematic case, even to the extent that the concept of the crystal shape (thickness) transform is no longer applicable. Detailed calculations of how the domain of validity of the kinematic theory is improved over that of the WPO approximation lie outside the scope of this preliminary investigation, in which we wish only to define a conservative estimate of the specimen thickness at which electron diffraction from protein crystals could be safely interpreted in terms of single-scattering theory.

The results of our present calculations are quite encouraging in that they show that the WPO approximation will be valid for proteins at significantly greater thicknesses than were found previously for simpler organic materials. For example, our previous calculation for anhydrous cytosine and for disodium 4-oxypyrimidine-2-sulfinate hexahydrate indicated that the thickness limitation would be two to four times less for small organic molecules than it is now found to be for a large complex protein molecule. This effect is not surprising, since a small unit cell in the beam direction, as occurs in the case of a simple structure, results in the precise superposition of atomic potentials as the thickness increases. When the projected potential in this way becomes too great, then the WPO approximation must necessarily fail. Of course, it is only the local deviations from the average projected potential (the 'inner' potential) that are important in determining the failure of the weak-phase-object approximation. In the case of a more complex structure, like a protein, the atomic potentials superimpose more or less at random, and it takes longer for the projected potential to exceed the limitations of the weak-phase-object approximation. Although this qualitative argument was expected to hold in advance, it was still necessary to do the actual calculations in order to determine the quantitative difference in specimen thickness at which the WPO approximation could be safely applied.

The results of our calculations have been further encouraging in that the thickness limitation of the WPO approximation corresponds rather closely to the finite thickness that one must in any case use for high-resolution imaging in order to keep within the depth of field of the objective lens. As a rule of thumb, the acceptable depth of field is given by

$$\Delta Z = d^2/2\lambda,$$

where d is the resolution and λ is the electron wavelength. At 3 Å resolution, $\Delta z = 120$ Å at 100 keV, 300 Å at 500 keV, and 500 Å at 1 MeV. Thus, it is a fortunate coincidence that it would be of no advantage in high-resolution imaging of proteins if the single-scattering approximation were valid to significantly greater thicknesses than has been determined in our calculations. The finite depth of field that exists for experimentally realistic accelerating voltages would, in any case, limit the specimen thickness to values quite similar to the ones that are apparently set by dynamical interaction effects. For the purpose of macromolecular crystallography, electrons in the intermediate high-voltage range, greater than 100 kV but less than 1 MV, seem to represent an optimum match in having as strong a scattering interaction as possible, in order to get a high yet directly interpretable level of image contrast, while having a sufficiently short wavelength to give a sufficiently large depth of field. Lower-energy electrons would, of course, restrict the specimen thickness due to dynamical effects and due to the depth of field; higher-energy electrons would increase the depth of field (without limit) but the limit due to dynamical effects cannot increase by any significant amount, owing to the relativistic limit on the electron velocity (Cowley, 1975).

This work was supported in part by National Institutes of Health grant GM 23325. We thank a referee for providing a translation of the paper by F.-K. Li.

References

AMOS, L. A., HENDERSON, R. & UNWIN, P. N. T. (1982). *Prog. Biophys. Mol. Biol.* **39**, 183–231.

CHIU, W. (1982). In *Electron Microscopy of Proteins*, edited by J. R. HARRIS, Vol. 2, pp. 233–259. New York: Academic Press.

COWLEY, J. M. (1975). *Diffraction Physics*. New York: American Elsevier Publishing Co.

COWLEY, J. M. & MOODIE, A. F. (1957). *Acta Cryst.* **10**, 609–619.

DORSET, D. L. (1984). *Ultramicroscopy* **13**, 311–324.

DORSET, D. L., JAP, B. K., HO, M.-H. & GLAESER, R. M. (1979). *Acta Cryst.* A**35**, 1001–1009.

DOYLE, P. A. & TURNER, P. S. (1968). *Acta Cryst.* A**24**, 390–397.

GLAESER, R. M. (1985). *Annu. Rev. Phys. Chem.* **36**, 243–275.

HENDERSON, R., BALDWIN, J. M., DOWNING, K. H., LEPAULT, J. & ZEMLIN, F. (1986). *Ultramicroscopy*, **19**, 147–178.

ISHIZUKA, K. & UYEDA, N. (1977). *Acta Cryst.* A**33**, 740–749.

JAP, B. K. & GLAESER, R. M. (1978). *Acta Cryst.* A**34**, 94–102.

JAP, B. K. & GLAESER, R. M. (1980). *Acta Cryst.* A**36**, 57–67.

JENG, J. W., CHIU, W., ZEMLIN, F. & ZEITLER, E. (1984). *J. Mol. Biol.* **175**, 93–97.

LI, F.-K. (1963). *Acta Phys. Sin.* **19**, 735–740.

MATHEWS, F. S., LEVINE, M. & ARGOS, P. (1972). *J. Mol. Biol.* **64**, 449–464.

WILSON, A. J. C. (1942). *Nature (London)*, **150**, 152.